

Myostatin promotes the wasting of human myoblast cultures through promoting ubiquitin-proteasome pathway-mediated loss of sarcomeric proteins

Sudarsanareddy Lokireddy,¹ Vincent Mouly,² Gillian Butler-Browne,² Peter D. Gluckman,³ Mridula Sharma,⁴ Ravi Kambadur,^{1,3} and Craig McFarlane³

¹School of Biological Sciences, Nanyang Technological University, Singapore; ²UPMC Université Paris 6, Institut de Myologie, Paris, France; ³Growth, Development and Metabolism Program, Singapore Institute for Clinical Sciences, Singapore; ⁴Yong Loo Lin School of Medicine, Department of Biochemistry, National University of Singapore, Singapore

Submitted 12 April 2011; accepted in final form 6 September 2011

Lokireddy S, Mouly V, Butler-Browne G, Gluckman PD, Sharma M, Kambadur R, McFarlane C. Myostatin promotes the wasting of human myoblast cultures through promoting ubiquitin-proteasome pathway-mediated loss of sarcomeric proteins. *Am J Physiol Cell Physiol* 301: C1316–C1324, 2011. First published September 7, 2011; doi:10.1152/ajpcell.00114.2011.—Myostatin is a negative regulator of skeletal muscle growth and in fact acts as a potent inducer of “cachectic-like” muscle wasting in mice. The mechanism of action of myostatin in promoting muscle wasting has been predominantly studied in murine models. Despite numerous reports linking elevated levels of myostatin to human skeletal muscle wasting conditions, little is currently known about the signaling mechanism(s) through which myostatin promotes human skeletal muscle wasting. Therefore, in this present study we describe in further detail the mechanisms behind myostatin regulation of human skeletal muscle wasting using an in vitro human primary myotube atrophy model. Treatment of human myotube populations with myostatin promoted dramatic myotubular atrophy. Mechanistically, myostatin-induced myotube atrophy resulted in reduced p-AKT concomitant with the accumulation of active dephosphorylated Forkhead Box-O (FOXO1) and FOXO3. We further show that addition of myostatin results in enhanced activation of atrogenin-1 and muscle-specific RING finger protein 1 (MURF1) and reduced expression of both myosin light chain (MYL) and myosin heavy chain (MYH). In addition, we found that myostatin-induced loss of MYL and MYH proteins is dependent on the activity of the proteasome and mediated via SMAD3-dependent regulation of FOXO1 and atrogenin-1. Therefore, these data suggest that the mechanism through which myostatin promotes muscle wasting is very well conserved between species, and that myostatin-induced human myotube atrophy is mediated through inhibition of insulin-like growth factor (IGF)/phosphoinositide 3-kinase (PI3-K)/AKT signaling and enhanced activation of the ubiquitin-proteasome pathway and elevated protein degradation.

myostatin-induced human muscle wasting; Forkhead Box-O; atrogenin-1; AKT; SMAD3

MYOSTATIN is a secreted growth factor, belonging to a large family of proteins collectively known as the transforming growth factor- β superfamily. Increased levels of myostatin are inhibitory to skeletal muscle myogenesis and as such genetic inactivation of *myostatin* in mice (21) or natural mutation of the *myostatin* gene in sheep (6), cattle (15, 22), and humans (28) results in a dramatic increase in skeletal muscle mass. In addition to negatively regulating skeletal muscle myogenesis, myostatin has been shown to act as a potent inducer of muscle

wasting. Systemic overexpression of myostatin in mice results in reduced body mass, loss of adipose and muscle tissue, and increased myofiber atrophy, all features consistent with cachexia syndrome (40). Furthermore, addition of recombinant myostatin protein to mouse C2C12 myotube cultures has been shown to promote severe myotubular atrophy. This has been revealed to be due to inhibition of insulin-like growth factor (IGF)/phosphoinositide 3-kinase (PI3-K)/AKT signaling resulting in enhanced FOXO1-mediated upregulation of components of the ubiquitin-proteasome pathway, including atrogenin-1 and muscle-specific E3 ubiquitin ligases muscle RING-finger 1 (MURF1) (20). In addition to studies involving animal models, myostatin has been linked with numerous human conditions that result in skeletal muscle wasting. Elevated myostatin expression is associated with patients undergoing acute and chronic human disuse atrophy (24), Type-II human muscle fiber atrophy (36), and muscle unloading as a result of unilateral lower limb suspension (12). Moreover elevated levels of myostatin are observed in individuals suffering from chronic illness such as end-stage liver disease (8), chronic obstructive pulmonary disease (23), and advancing age-related muscle wasting or sarcopenia (18, 37). Intramuscular and serum levels of a myostatin-immunoreactive protein are also increased in HIV-infected men undergoing skeletal muscle wasting when compared with healthy controls (10).

In addition, a recent paper by Trendelenburg et al. (34) demonstrated that treatment of human myotube cultures with myostatin resulted in the development of myotube atrophy, which is consistent with what is observed in rodent models (20). Trendelenburg et al. (34) suggests that the myostatin-mediated atrophy was due to inhibition of myogenic gene expression and reduced protein synthesis, through blockade of AKT/TORC1/p70S6K signaling. Trendelenburg et al. further suggested that the myotube atrophy resulted primarily from reduced protein synthesis, as opposed to increased protein degradation via induction of atrogenes and the ubiquitin-proteasome pathway (34), as previously shown (20).

Here we have studied in detail the mechanism(s) of action of myostatin during human myotube atrophy to clarify the role of myostatin in regulating myotube size and muscle protein degradation in human skeletal muscle. Our results reveal that myostatin-mediated human myotube atrophy is associated with sarcomeric protein loss, inhibition of AKT signaling, and enhanced expression of the ubiquitin E3 ligases atrogenin-1 and MURF1. Furthermore, we found that SMAD3 signaling is critical for myostatin-dependent upregulation of FOXO1 and atrogenin-1 expression and subsequent sarcomeric protein degradation through the ubiquitin-proteasome pathway.

Address for reprint requests and other correspondence: C. McFarlane, Growth, Development and Metabolism Program, Singapore Institute for Clinical Sciences, Brenner Centre for Molecular Medicine, 30 Medical Dr., Singapore, 117609 (e-mail: craig_mcfarlane@sics.a-star.edu.sg).

MATERIALS AND METHODS

Myostatin purification. Human recombinant myostatin protein (hMstn) was cloned, expressed, and purified from *Escherichia coli* as described (29). Myostatin-overexpressing Chinese hamster ovary (CHO) cells (kindly provided by Dr. Se-Jin Lee) and purification of murine myostatin (CHO-myostatin; CM) from these cells have been described (21). Human primary myoblast cultures were treated with CM at a final concentration of 10 ng/ml for all relevant experiments.

Cell culture. The human primary myoblast cell strain used in the present study is designated as hMb15 (isolated from a 15-yr-old healthy subject, provided by the BTR tissue bank affiliated with EuroBioBank)(3, 7, 13). Human myoblast cultures were maintained at 37°C/5% CO₂ in proliferation medium, which consists of Dulbecco's modified Eagle medium (DMEM; Invitrogen, Carlsbad, CA) supplemented with 20% fetal bovine serum (FBS; Invitrogen), 10% horse serum (HS; Invitrogen), and 1% chicken embryo extract (CEE; US Biological, Swampscott, MA). To assess the ability of hMstn to induce myotubular atrophy, human myoblasts were plated on Thermanox coverslips (Nunc, Roskilde, Denmark) at a density of 25,000 cells/cm² and induced to differentiate under low serum conditions (DMEM 2% HS). After 72 h differentiation, the cultures were treated for an additional 24 h in differentiation media without or with 5 µg/ml hMstn. The cultures were then fixed with ethanol-formaldehyde-glacial acetic acid (20:2:1) and stained with Gill's hematoxylin and 1% eosin. Myotube area was assessed microscopically using the Image-Pro Plus analysis software package (MediaCybernetics, Bethesda, MD), with individual myotube area assessed for all myotubes present in 10 random images taken from three coverslips per treatment.

MG132 treatment. To study the role of proteasome-mediated protein degradation on hMstn-induced human myotube atrophy, hMb15 human myoblasts were differentiated (as described above) for 96 h followed by an additional 24 h in the absence or presence of hMstn (5 µg/ml). The proteasome inhibitor MG132 (Sigma-Aldrich, St. Louis, MO) was added to the human myotube cultures at a concentration of 10 µM during the final 10 h of hMstn treatment only. Cells were then harvested for protein isolation and subsequent Western blot analysis.

Assessment of protein degradation in hMb15 myotubes. hMb15 myotubes were incubated with 5 µCi/ml [³H]tyrosine for 36 h to label cellular proteins, according to the previously mentioned protocol (11). The medium was then switched to chase media containing 2 mM of unlabeled tyrosine for 2 h to prevent the reincorporation of labeled [³H]tyrosine. Myotubes were then incubated with fresh chase media in the absence (dialysis buffer) or presence of hMstn for 24 h, with the protease inhibitor MG132 added 12 h before media sample collection. After collection, the medium was precipitated with 10% TCA and centrifuged at 12,000 rpm for 10 min at 4°C. Acid-soluble radioactivity was subsequently measured using a liquid scintillation counter (1450 LSC and Luminescence counter; PerkinElmer Life Sciences, Waltham, MA) and reflects the amount of prelabeled long-lived protein degraded. The values are normalized to the total radioactivity initially incorporated, and the graph represents the level of protein degradation expressed as a percentage of initial.

Assessment of protein synthesis in hMb15 myotubes. Total protein synthesis was assessed by measuring the rate of [³H]tyrosine incorporation in myotubes, as per the previously published protocol (35). hMb15 myotubes (96 h differentiated) were treated in the absence (dialysis buffer) or presence of hMstn for 24 h, followed by incubation with medium containing 5 µCi/ml [³H]tyrosine for 2 h. After incubation, the medium was discarded and the myotubes were washed twice with PBS before addition of 1 ml 10% TCA to precipitate total proteins. Total cell lysates were then collected and centrifuged at 1,200 rpm for 10 min at 4°C. The resulting pellet was washed with 95% ethanol and dissolved in 0.1 N NaOH at 25°C for 2 h with rocking. These samples were analyzed for total radioactivity using a liquid scintillation counter (1450 LSC and Luminescence counter;

PerkinElmer) with the level of radioactivity normalized to total protein content. Results were expressed as counts per minute per milligram of protein for each well, normalized to the vehicle control.

Specific inhibitor of SMAD3 treatment. To study the role of SMAD3 signaling during hMstn-mediated human myotube atrophy, hMb15 human myoblasts were differentiated (as described above) for 96 h followed by a further 24 h in the absence (0.05% DMSO) or presence of the SMAD3-specific inhibitor SIS3 (10 µM; Sigma-Aldrich) with or without hMstn (5 µg/ml). Cells were then harvested for protein isolation and subsequent Western Blot analysis.

siRNA-mediated knockdown of SMAD3. hMb15 human myoblasts were seeded in six-well plates at a density of 25,000 cells/cm². After a 24-h attachment period, the cells were transfected with 30 nM of each specific MISSION predesigned small interfering RNA (siRNA, Sigma-Aldrich) using Lipofectamine 2000 reagent (Invitrogen) as per the manufacturer's guidelines. The myoblasts were then induced to differentiate under low serum conditions (DMEM 2% HS) for 72 h followed by a further 24 h in differentiation media with or without 3 µg/ml hMstn. Cells were then harvested for protein isolation and subsequent Western blot analysis. Details of each specific MISSION predesigned siRNAs are provided below: MISSION siRNA Universal Negative Control (SIC001; Scrambled siRNA); human SMAD3 siRNA-1, GAG UUC GCC UUC AAU AUG AdT dT; and human SMAD3 siRNA-2, CAU GGA CGC AGG UUC UCC AdT dT.

Immunoprecipitation studies. For myosin heavy chain (MYH) and myosin light chain (MYL) immunoprecipitation, hMb15 primary myoblasts were differentiated for 96 h then incubated for an additional 24 h in the absence or presence of hMstn (5 µg/ml). Cultures were then harvested in 1 ml of RIPA buffer (50 mM NaF, 0.5% Na deoxycholate, 0.1% SDS, 1% IGEPAL, 1.5 mM Na₃VO₄ and complete protease inhibitor; Roche Molecular Biochemicals, Indianapolis, IN) and centrifuged to remove cell debris. Bradford reagent (Bio-Rad, Hercules, CA) was used to estimate total protein content to ensure equal loading. Before immunoprecipitation, 250 µg of total protein was precleared using 25 µl of a 50% Protein A-agarose slurry for 1 h at 4°C. Immunoprecipitation of MYH and MYL was performed by incubating the precleared lysate with 2 µg of purified mouse monoclonal anti-MYH or purified mouse monoclonal anti-MYL, respectively, for 2 h at 4°C. Protein A-agarose (Invitrogen) (50 µl of 50% percent), washed twice with RIPA buffer, was added for 1 h at 4°C, followed by centrifugation to pellet immunoprecipitated complexes. Pellets were washed four times with cold PBS, resuspended in 50 µl of 1× NuPAGE sample buffer (Invitrogen), and boiled for 5 min. Immunoprecipitation samples were fractionated by SDS-PAGE and transferred to nitrocellulose membrane by electroblotting for subsequent Western blot analysis.

Western blot and analysis. Preparation of protein extracts from myoblasts and subsequent Western blot analysis have been previously described in detail (33). Western blots were quantified by densitometric analysis using the GS-800 densitometer (Bio-Rad). Western blots presented in this study are representative of at least two independent experiments. Details of the antibodies used for Western analysis and immunoprecipitation studies are provided below: mouse monoclonal anti-MYL [T14; Developmental Studies Hybridoma Bank (DSHB), Iowa City, IA]; mouse monoclonal anti-MYH (MF-20; DSHB); rabbit polyclonal anti-pSMAD2/3 (sc-11769-R; Santa Cruz Biotechnology, Santa Cruz, CA); goat polyclonal anti-SMAD2/3 (sc-6032; Santa Cruz Biotechnology); rabbit polyclonal anti-atrogin-1 (gifted by Dr Esther Latres); mouse monoclonal anti-MURF1 (gifted by Dr Esther Latres); mouse monoclonal anti-ubiquitin (sc-8017; Santa Cruz Biotechnology); rabbit polyclonal anti-FOXO1 (sc-11350; Santa Cruz Biotechnology); rabbit polyclonal anti-p-FOXO1 (sc-101681; Santa Cruz Biotechnology); rabbit monoclonal anti-FOXO3 (ab53287; Abcam, Cambridge, MA); rabbit polyclonal anti-p-FOXO3 (sc-101689; Santa Cruz Biotechnology); rabbit polyclonal anti-AKT (sc-8312; Santa Cruz Biotechnology); rabbit polyclonal anti-p-AKT (sc-

7985-R; Santa Cruz Biotechnology) and purified mouse monoclonal anti-tubulin antibody (T-9026; Sigma-Aldrich).

Statistical analysis. Single comparisons were made using two-tail Student's *t*-tests and one-way ANOVA. Data are expressed as means \pm SD, and *P* values <0.01 were considered significant. Experimental replicates are described in relevant figure legends.

RESULTS

Treatment with myostatin results in dramatic myotube atrophy in human myoblast cell strains. Treatment of 72 h differentiated hMb15 human myotube cultures with *E. coli*-produced hMstn resulted in dramatic myotubular atrophy (Fig. 1A). Specifically, we observed a \sim 70% decrease in the number of larger myotubes ($\geq 15,000 \mu\text{m}^2$) concomitant with a \sim 83% increase in the number of smaller ($< 10,000 \mu\text{m}^2$) myotubes in the hMb15 cell strain following treatment with hMstn (Fig. 1, B and C).

Treatment of human myotube cultures with hMstn induces the loss of sarcomeric proteins and upregulation of components of the ubiquitin-proteasome pathway. Western blot analysis of MYH and MYL sarcomeric protein expression in hMb15 human myotube cultures treated with hMstn (Fig. 2A) revealed decreased expression of both MYH and MYL in hMstn-treated cells at all time points analyzed, consistent with the myotubular atrophy observed following treatment with hMstn. To independently confirm the functionality of the hMstn recombinant protein, we also treated human myotube cultures with eukaryotic-produced CHO cell-secreted recombinant myostatin protein (CM). Much akin to hMstn treatment, addition of CM also led to reduced expression of both MYH and MYL (Fig. 2B). Next, we analyzed the expression of atrogen-1 and MURF1, two important ubiquitin E3 ligases, which have proved to be robust markers for several forms of skeletal muscle wasting (17). The results revealed a significant increase in the expression of both atrogen-1 and MURF1 in the

hMb15 human myoblast cell strain following treatment with hMstn (Fig. 2A). Furthermore, induction of myotubular atrophy through treatment with CM also resulted in an increase in the abundance of atrogen-1 and MURF1 (Fig. 2B). These data demonstrate that hMstn-induced human myotubular atrophy results in a loss of sarcomeric proteins, which we suggest may be due to increased protein degradation through the proteasomal system.

Myostatin-mediated protein degradation is dependent on the activity of the proteasome. Treatment of human myotubes cultures with hMstn resulted in increased protein degradation, as determined through quantifying the loss of [^3H]tyrosine-labeled cellular proteins after hMstn treatment (Fig. 2C). Moreover, addition of the proteasome inhibitor MG132, which has been shown to block proteasome-mediated protein degradation and thereby significantly increase protein content during atrophy (5, 31), prevented the elevated proteolysis observed following addition of hMstn (Fig. 2C). Thus hMstn treatment results in enhanced protein degradation, which is mediated, at least in part, through the action of the ubiquitin-proteasome pathway.

To confirm whether or not hMstn-mediated degradation of sarcomeric proteins occurs via the proteasomal system, MG132 was added to hMb15 myotube cultures in the presence or absence of hMstn (Fig. 2D). As expected addition of hMstn resulted in the loss of both MYH and MYL; however, blockade of the proteasomal system, through addition of MG132, prevented hMstn-mediated loss of both MYH and MYL (Fig. 2D). Importantly, addition of MG132 had no appreciable effect on either the basal expression of atrogen-1 and MURF1 or on the ability of hMstn to enhance atrogen-1 and MURF1 expression in the human myotube cultures (Fig. 2D).

To determine whether or not hMstn-mediated loss of MYH and MYL resulted from enhanced ubiquitination, MYH and

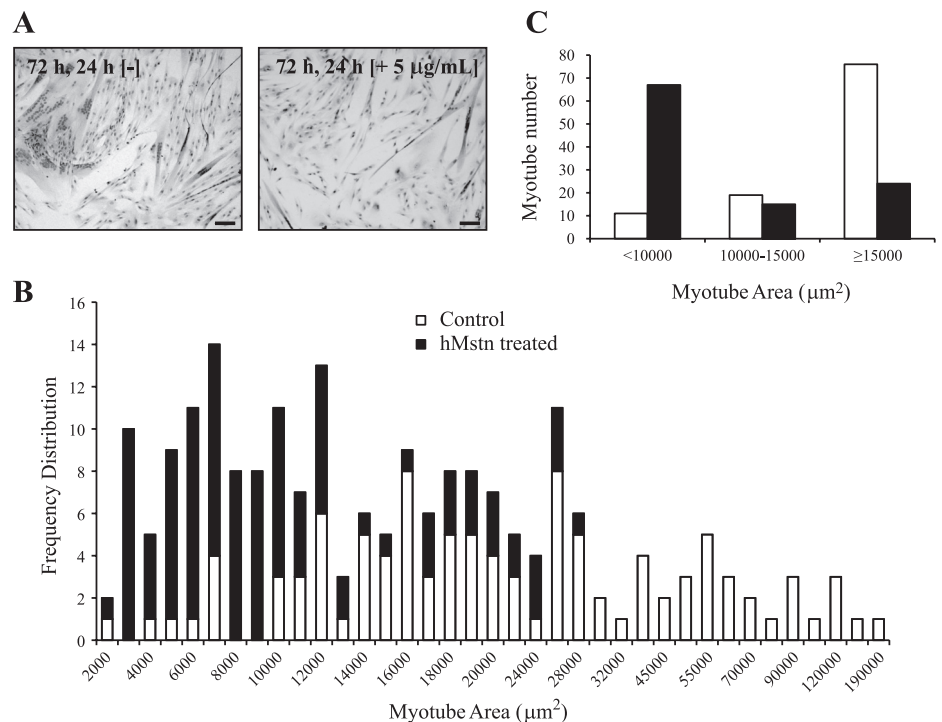


Fig. 1. Addition of human recombinant myostatin protein (hMstn) results in the development of severe human myotube atrophy. A: representative images of hMb15 human myoblasts differentiated for 72 h, followed by an additional 24 h with [72 h, 24 h (+5 $\mu\text{g}/\text{ml}$)] or without [72 h, 24 h (-)] hMstn (5 $\mu\text{g}/\text{ml}$). Myotube cultures were fixed and stained with Gill's hematoxylin and eosin. Scale bar represents 50 μm . B: frequency distribution of myotube area (μm^2) over 3 coverslips per treatment for the hMb15 human cell strain. C: number of myotubes, sorted based on myotube area, into small ($< 10,000 \mu\text{m}^2$), medium ($10,000 \mu\text{m}^2$ to $15,000 \mu\text{m}^2$), or large ($\geq 15,000 \mu\text{m}^2$) groupings. Myotube area was assessed for all myotubes present in 10 random images per coverslip per treatment.

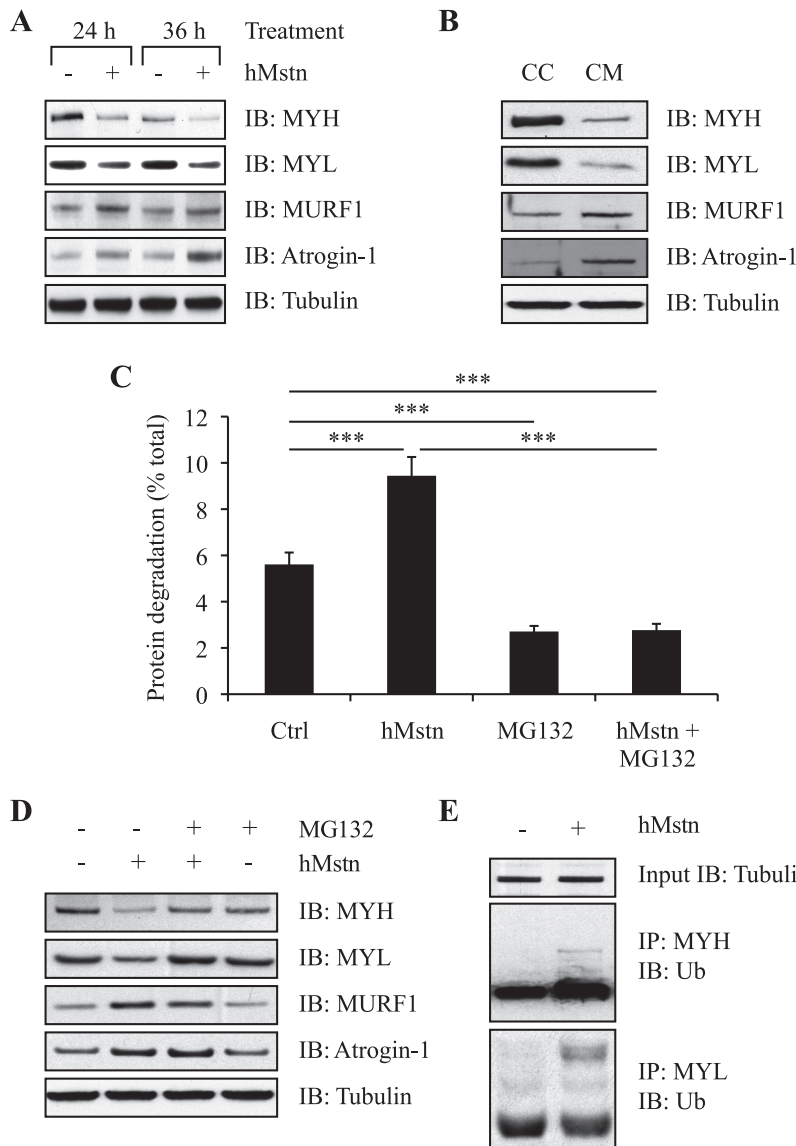


Fig. 2. Myostatin-induced human myotube atrophy results in the loss of sarcomeric proteins in an ubiquitin-proteasome pathway-dependent manner. Human myoblast cultures were differentiated for 72 h followed by treatment with (+) or without (-) hMstn (5 µg/ml) for a further period of 24 or 36 h differentiation. **A**: Western blot analysis of the expression of MYH, MYL, MURF1, and atrogen-1 in hMb15 human myotubes following treatment with hMstn. **B**: Western blot analysis of MYH, MYL, MURF1, and atrogen-1 expression in hMb15 human myotubes following 24 h treatment without (CC) or with eukaryotic-produced CHO cell-secreted recombinant myostatin protein (CM). **C**: Western blot analysis of MYH, MYL, MURF1, and atrogen-1 expression in hMb15 myotubes treated with (+) or without (-) hMstn in the presence (+) or absence (-) of the proteasome inhibitor MG132. **D**: sarcomeric proteins were immunoprecipitated using pan-MYH- and pan-MYL-specific antibodies and subjected to Western blot using a specific anti-ubiquitin antibody. The visible mobility shift (ladder profile) of MYH and MYL proteins as a result of hMstn treatment is consistent with ubiquitination. The expression of tubulin was assessed to ensure equal loading of samples. **E**: hMstn increases protein degradation in differentiated myotubes. Differentiated myotubes were incubated with [³H]tyrosine for 36 h and then treated with either hMstn or MG132 or a combination of both. Medium was collected at 24 h, and the amount of degraded [³H]tyrosine-labeled protein was expressed as a percentage of the initial amount of [³H]tyrosine added. ****P* < 0.001. Error bars represent means ± SD (*n* = 4).

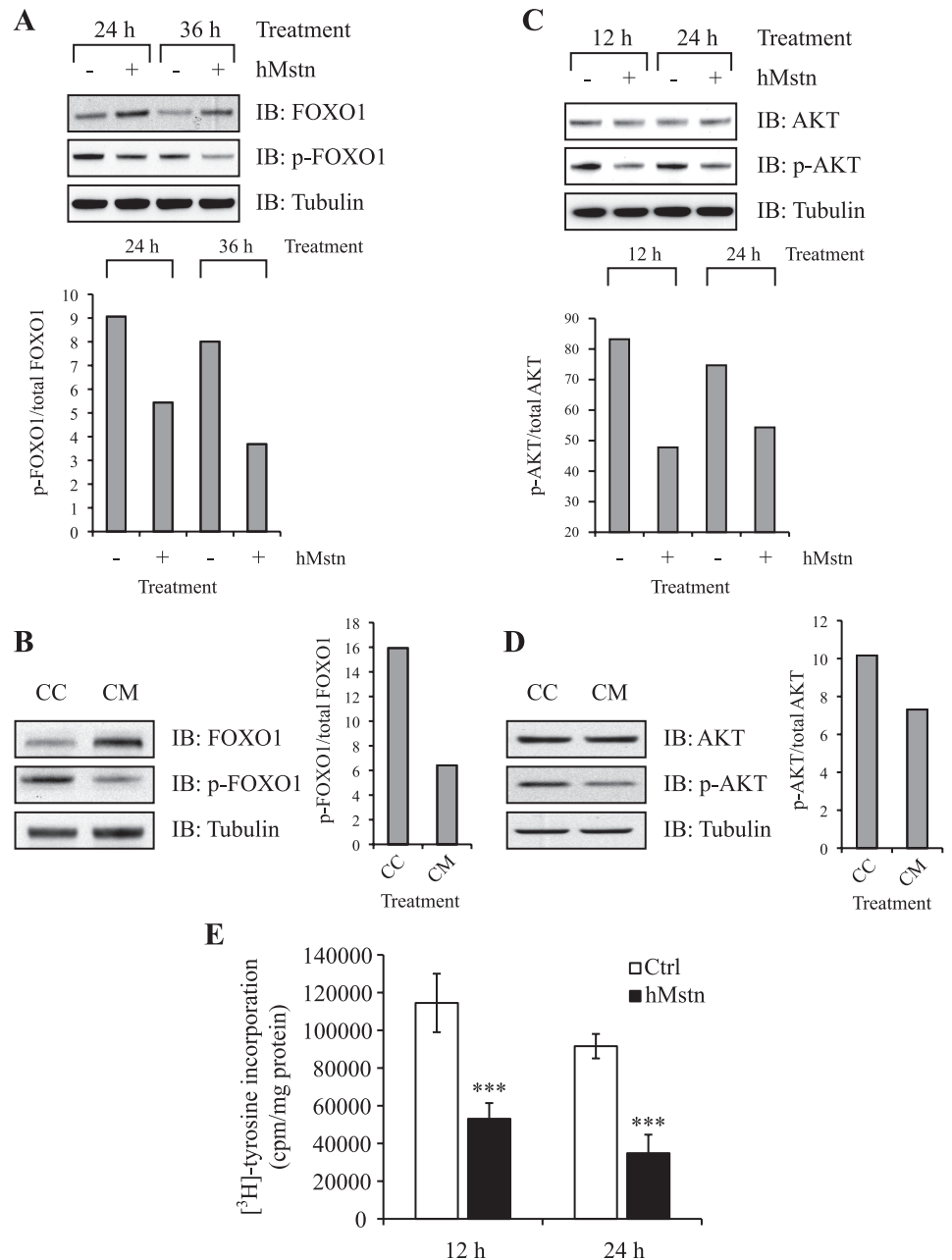
MYL isoforms were specifically immunoprecipitated using pan-MYH- and pan-MYL-specific antibodies and analyzed by Western blot for the coimmunoprecipitation of ubiquitin using a specific anti-ubiquitin antibody (Fig. 2E). Western blot analysis of ubiquitin that coimmunoprecipitated with MYH and MYL from human myotube cultures treated with hMstn revealed increased ubiquitination of both MYH and MYL following treatment with hMstn, with a characteristic ladder profile, consistent with ubiquitination, visible only in hMstn-treated human myotube cultures (Fig. 2E). These data suggest that hMstn promotes human myotubular wasting and protein degradation through increased ubiquitination of sarcomeric proteins.

Addition of myostatin antagonizes the IGF-1 hypertrophy signaling pathway and reduces protein synthesis during the induction of human myotubular atrophy. The dephosphorylation and thus activation of FOXO transcription factors, such as FOXO1, is critical to the ability of FOXO factors to induce skeletal muscle wasting through regulation of so called atrophy-related genes or “atrogenes,” which include the well-

characterized ubiquitin E3 ligase atrogen-1 (26, 30). Therefore, we next analyzed the expression of total FOXO1 and p-FOXO1 in human myotube populations following treatment with hMstn. Western blot analysis of FOXO1 and p-FOXO1 protein expression in hMb15 myotube cultures treated for a period of 24 and 36 h with hMstn revealed increased expression of total FOXO1 and decreased abundance of p-FOXO1, at 24 and 36 h in the hMb15 cell strain following treatment with hMstn (Fig. 3A). Similarly, when we treated hMb15 human myotube cultures with CM, we also observed increased total FOXO1 and reduced p-FOXO1 (Fig. 3B). Therefore, treatment with either hMstn or CM resulted in the accumulation of dephosphorylated and thus active FOXO1 in the human myoblast cultures.

Because the IGF/PI3-K/AKT pathway promotes the phosphorylation and subsequent inhibition of FOXO transcription factors, we next analyzed whether or not myostatin signaling antagonizes the action of the IGF/PI3-K/AKT pathway during myostatin-mediated human skeletal muscle wasting. Consistent with reversal of canonical IGF/PI3-K/AKT signaling, we

Fig. 3. Myostatin-induced human myotube atrophy results in enhanced activation of Forkhead Box-O (FOXO1) and inhibition of insulin-like growth factor (IGF)/phosphoinositide 3-kinase (PI3-K)/AKT signaling. Human myoblast cultures were differentiated for 72 h followed by treatment with (+) or without (-) hMstn (5 μ g/ml), or without (CC) or with CM for a further period of 12, 24, or 36 h differentiation. *A* and *B*: Western blot analysis of FOXO1 and p-FOXO1 expression in hMb15 human myotube cultures following treatment with either hMstn (*A*) or CM (*B*). *C* and *D*: Western blot analysis of AKT and p-AKT expression in hMb15 human myotube cultures following treatment with either hMstn (*C*) or CM (*D*). The expression of tubulin was assessed to ensure equal loading of samples. Graphs represent densitometric analysis of Western blots [FOXO1, p-FOXO1 (*A* and *B*), AKT and p-AKT (*C* and *D*)], normalized to tubulin expression. The abundance of p-FOXO1 is expressed as a proportion of total FOXO1 (*A* and *B*) and the abundance of p-AKT is expressed as a proportion of total AKT (*C* and *D*). *E*: hMstn decreases protein synthesis in differentiated myotubes. Differentiated myotubes were treated with hMstn for 24 h, followed by a further incubation with [3 H]tyrosine for 2 h. Total cell lysates were collected and the level of protein synthesis, as measured via [3 H]tyrosine incorporation, was assessed and expressed as counts per minute (cpm) normalized to total protein content (cpm/mg protein). *** $P < 0.001$. Error bars represent means \pm SD ($n = 6$).



found that treatment with either hMstn or CM reduced the abundance of p-AKT in the hMb15 human myotube cultures (Fig. 3, *C* and *D*). Previously published data have demonstrated that treatment with excess myostatin inhibits protein synthesis (32). Moreover, reduced AKT/mammalian target of rapamycin (mTOR) protein synthesis signaling and increased atrophy was observed following overexpression of myostatin in muscle (1) and in response to treatment of myotubes with recombinant myostatin protein (34). As we observed reduced p-AKT (Fig. 3, *C* and *D*) we next assessed whether or not hMstn treatment resulted in reduced protein synthesis in the human myotube cultures. As shown in Fig. 3*E*, treatment of human myotubes cultures with hMstn resulted in reduced protein synthesis, as measured through [3 H]tyrosine incorporation, at both 12 and 24 h treatment (Fig. 3*E*).

Therefore, these data suggest that myostatin promotes human skeletal muscle wasting through both inhibiting protein synthesis as well as antagonising IGF/PI3-K/AKT signaling, thereby blocking AKT-mediated phosphorylation of FOXO1, leading to increased expression of both activated FOXO1 and FOXO1 downstream target genes, including atrogin-1.

Myostatin signals through SMAD3 to regulate atrogin-1 and FOXO1 during myostatin-induced human myotube atrophy. To determine whether or not SMAD3 signaling is important in hMstn-mediated human myotube atrophy, hMb15 human myotube cultures were treated with hMstn in the presence or absence of SIS3, which has previously been shown to specifically inhibit SMAD3 function through suppressing SMAD3 phosphorylation (14). As expected, treatment with SIS3 resulted in both a reduction in endogenous p-SMAD3 expres-

sion, when compared with untreated control, and also blocked the ability of hMstn to promote phosphorylation of SMAD3 in the hMb15 myotube cultures (Fig. 4A). While addition of hMstn to control treated (0.05% DMSO) hMb15 myotube cultures resulted in an increase in the expression of atrogen-1, FOXO1, MURF1, and FOXO3, concomitant with reduced expression of MYH (Fig. 4, B and C), addition of SIS3 to hMstn-treated hMb15 myotube cultures blocked the ability of

hMstn to enhance the expression of atrogen-1 and FOXO1 and also prevented loss of MYH (Fig. 4B). Similarly, knockdown of SMAD3 through transfection of SMAD3-specific siRNA also interfered with hMstn-mediated upregulation of FOXO1 and atrogen-1 and subsequent loss of MYH (Fig. 4D). Interestingly, hMstn treatment was still able to enhance the protein expression of MURF1 and FOXO3 despite the inhibition of SMAD3 through SIS3 treatment (Fig. 4C), suggesting that

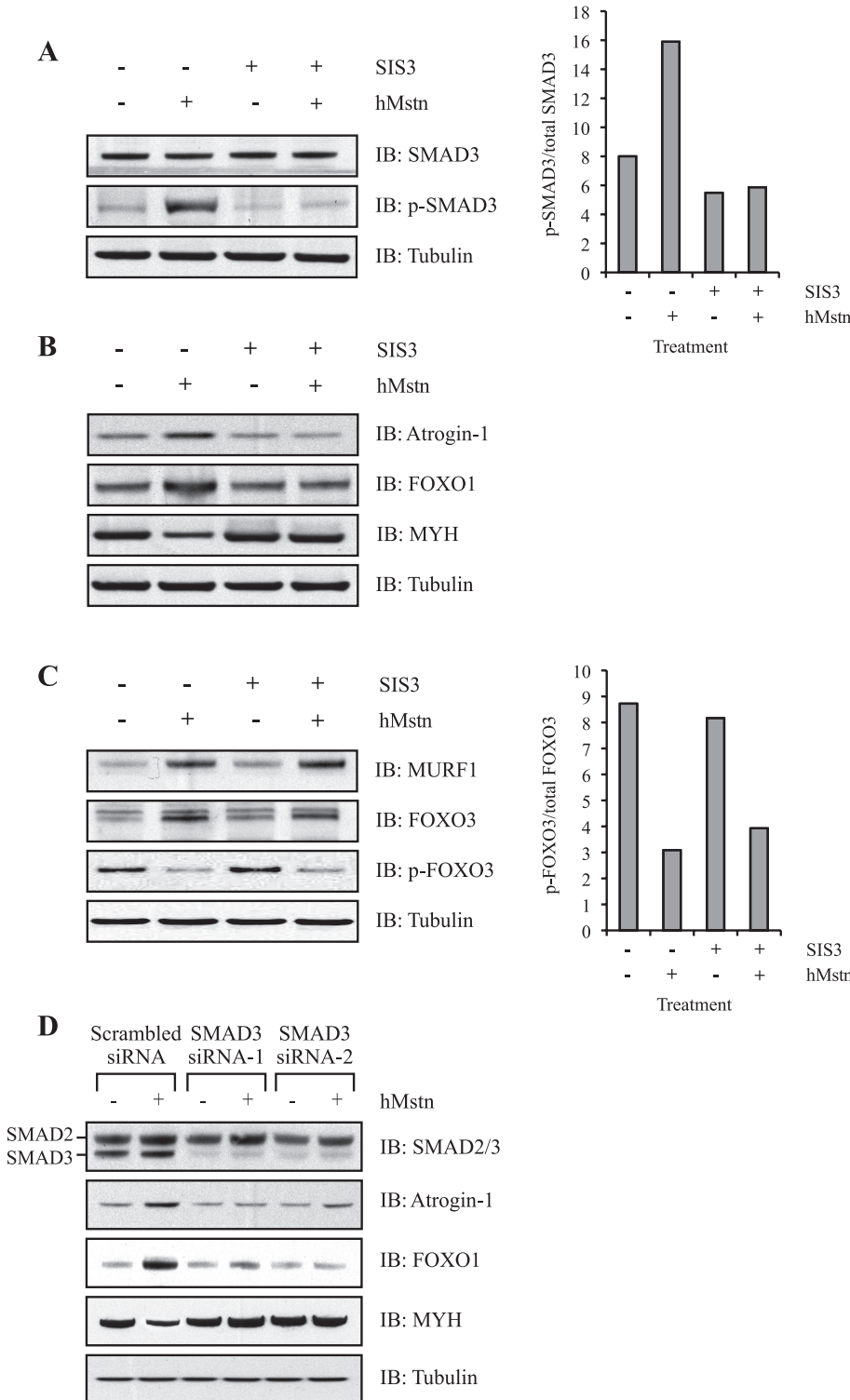


Fig. 4. The SMAD3 signaling pathway plays a critical role during myostatin-induced human myotube atrophy. Human myoblast cultures were differentiated for 72 h followed by treatment with (+) or without (-) hMstn (5 μg/ml) in the presence (+) or absence (-) of the SMAD3-specific inhibitor SIS3 for a further period of 24 h differentiation. Western blot analysis of the expression of SMAD3 and p-SMAD3 (A); atrogen-1, FOXO1, and MYH (B); and MURF1, FOXO3, and p-FOXO3 (C) following treatment with (+) or without (-) hMstn in the presence (+) or absence (-) of SIS3. The abundance of p-SMAD3 is expressed as a proportion of total SMAD3 (A) and the abundance of p-FOXO3 is expressed as a proportion of total FOXO3 (C). D: Western blot analysis of the expression of SMAD2/3, atrogen-1, FOXO1, and MYH following treatment with (+) or without (-) hMstn in hMb15 myoblasts transfected with Universal Negative Control [Scrambled small interfering RNA (siRNA)] and SMAD3-specific siRNAs (SMAD3 siRNA-1 and SMAD3 siRNA-2). The expression of tubulin was assessed to ensure equal loading of samples.

hMstn requires active SMAD3 signaling to regulate both FOXO1 and atrogenin-1 and for regulation of sarcomeric protein expression, whereas SMAD3 is dispensable for hMstn regulation of FOXO3 and MURF1.

DISCUSSION

In this present study, we have assessed the effect of the pro-cachectic growth factor myostatin on human skeletal muscle myotube cultures, in an effort to gain better understanding of the mechanism through which myostatin promotes skeletal muscle wasting (Fig. 5). Using a human primary myoblast culture model, *E. coli*-produced hMstn, and eukaryotic-produced CHO cell-secreted recombinant myostatin protein (CM), we show that human myostatin promotes human myotube wasting by activating the ubiquitin-proteasome pathway. Consistent with studies using murine myoblast models (20), hMstn and CM treatment induced the expression of atrogenin-1 and MURF1 (Fig. 2, A and B), two muscle-specific ubiquitin E3 ligases shown to be upregulated in numerous form of muscle wasting (17). Myostatin-induced human myotube atrophy further resulted in the loss of critical sarcomeric proteins in the human myotube cultures, which was due to the action of the ubiquitin-proteasome pathway as hMstn treatment resulted in enhanced ubiquitination of both MYH and MYL isoforms (Fig. 2E). Moreover, MG132-mediated blockade of hMstn-induced protein degradation resulted in a rescue of both MYH and MYL expression (Fig. 2, C and D). Targeted degradation of sarcomeric proteins, such as MYH and MYL, through the ubiquitin-proteasome pathway is not a new concept. In fact, treatment of C2C12 myotube cultures with the artificial glucocorticoid dexamethasone (Dex) has been recently demonstrated to promote wasting through MURF1-dependent degradation of MYH and MYL isoforms (5). Although we find that hMstn treatment results in the loss of MYH and MYL, unlike Dex-induced myotube atrophy, myostatin appears to preferentially signal through atrogenin-1, not MURF1, to promote the loss of sarcomeric proteins in human myotube cultures. In fact we demonstrated that, in human cultures with impaired SMAD3 signaling, the expression of MURF1 remained elevated following hMstn treatment; however, loss of SMAD3 signaling prevented hMstn-mediated upregulation of atrogenin-1 and FOXO1 and importantly also prevented hMstn-mediated loss of MYH (Fig. 4). Taken together, these data further suggest that the function of atrogenin-1 and MURF1 may vary in response to different cachectins. In support, although both atrogenin-1 and MURF1 are upregulated in response to Dex treatment (5, 26), absence of *MuRF1*, not *Atrogenin-1*, protects against Dex-induced muscle loss (2).

Previously published results indicate that myostatin is able to activate FOXO1 during murine myotubular atrophy (20). However, the current results reveal that, in addition to FOXO1, hMstn was also able to induce FOXO3 during human myotube atrophy. Interestingly, unlike FOXO1, hMstn was still able to enhance FOXO3 expression in the absence of SMAD3 (Fig. 4C). Since myostatin-induced human myotube atrophy has been shown to result in enhanced phosphorylation of SMAD2 (34), we suggest that hMstn regulation of FOXO3 in the human myotube cultures may be mediated through a SMAD2-dependent mechanism. It is noteworthy to mention that FOXO3 has been recently shown to promote autophagy in skeletal muscle

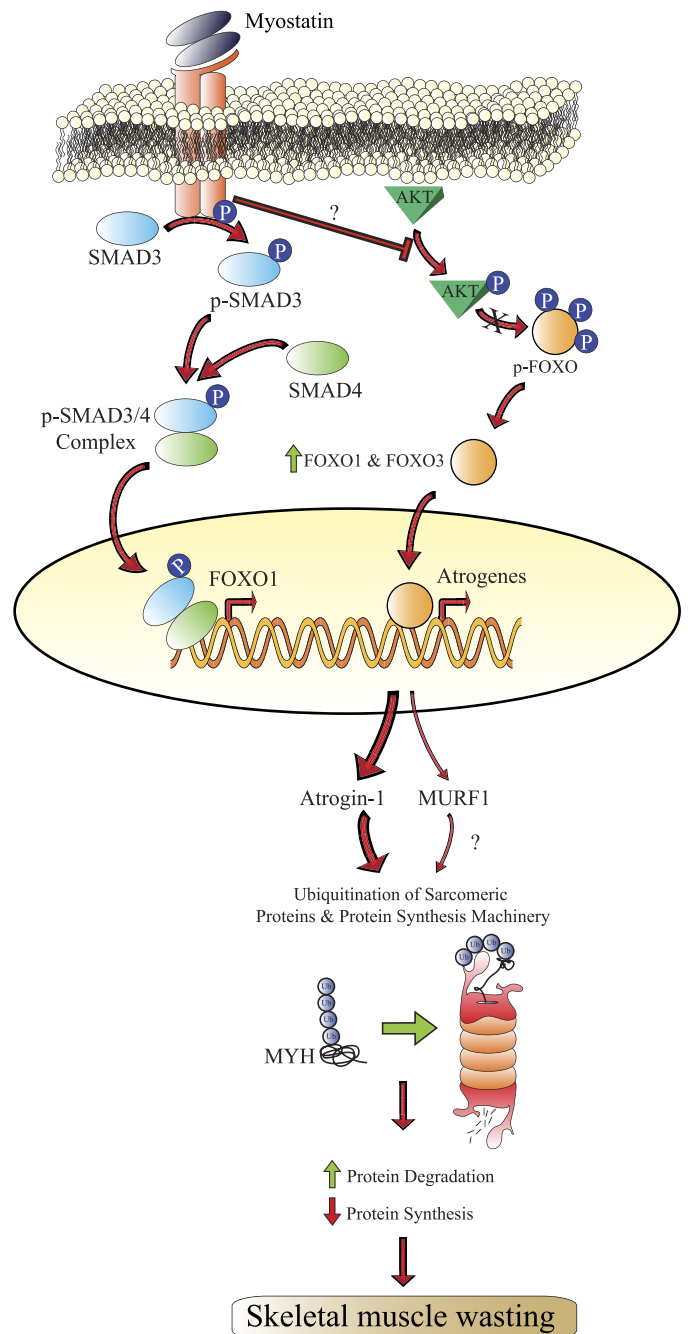


Fig. 5. Myostatin promotes dramatic wasting in human myotube cultures via the ubiquitin-proteasome pathway. Myostatin-mediated human myotube atrophy results in enhanced FOXO1 expression via a mechanism involving canonical SMAD3 signaling. Through inhibition of AKT phosphorylation, myostatin treatment results in the accumulation of active dephosphorylated FOXO transcription factors, which further results in the activation of FOXO target genes, including atrogenin-1 and MURF1, leading to the ubiquitination of critical sarcomeric proteins and most likely protein synthesis machinery (eIF3-f), increased protein degradation, reduced protein synthesis, and the development of myotubular atrophy in the human myotube cultures. Arrows represent stimulation and blunt-ended lines represent inhibition.

through regulating the expression of autophagy-related genes such as *LC3* and *Bnip3* (19, 38). Therefore, enhanced activation of FOXO3 in response to myostatin treatment may promote autophagy in the human myotube atrophy model; how-

ever, further work will need to be performed to verify a role for myostatin regulation of FOXO3 and the induction of autophagy during skeletal muscle wasting.

In addition to the increased expression of FOXO3, we also found a SMAD3-independent increase in MURF1 expression following treatment with hMstn (Fig. 4C), thus we propose that FOXO3 may be important for myostatin regulation of MURF1 expression. In fact, previous studies have shown that activation of FOXO3 is linked with increased abundance of MURF1, enhanced protein degradation, and development of skeletal muscle wasting (4, 25, 39). Although we found enhanced accumulation of active dephosphorylated FOXO3 and elevated MURF1 expression following treatment with hMstn, the data presented here suggest that myostatin-mediated degradation of sarcomeric proteins during human myotube atrophy occurs predominantly via a FOXO1/atrogin-1 mechanism rather than through FOXO3/MURF1. Therefore, further work will need to be performed to clarify the role of MURF1 in myostatin-mediated human muscle wasting.

Previously published results by Taylor et al. (32) indicate that treatment of C2C12 myotubes with excess myostatin results in decreased protein synthesis, with no appreciable change in the rate of protein degradation. Furthermore, a recent paper by Trendelenburg et al. (34) provides evidence to suggest that myostatin-mediated human myotube atrophy results from inhibition of the AKT/TORC1/p70S6K protein synthesis-signaling pathway rather than from increased protein degradation. In agreement with previously published reports, we also found reduced protein synthesis as well as reduced phosphorylation of AKT and the AKT downstream target FOXO1 following treatment of human myotubes cultures with either hMstn or CM (Fig. 3). However, in contrast to the work of Trendelenburg et al. we found elevated expression of the ubiquitin E3 ligases atrogin-1 and MURF1. Moreover, we also observed enhanced ubiquitination and subsequent proteasome-dependent protein degradation and loss of sarcomeric proteins during hMstn-induced human myotube wasting (Fig. 2). We suggest that the disparity between what we observed in the present study and the published data of Taylor et al. and Trendelenburg et al. may be due to the different model system used as well as the differences in recombinant myostatin protein used. Nevertheless, these data presented in this current study are in agreement with recently published work, which demonstrates the capacity for myostatin signaling to promote atrogin-1 promoter activity (27), as well as previously published work from our lab demonstrating enhanced protein ubiquitination and elevated expression of atrogin-1 and MURF1 following addition of excess myostatin to mouse model systems (20). Absence of myostatin has also been shown to prevent upregulation of atrogin-1 and MURF1 as well as the increased 20S proteasome activity observed during Dex-induced muscle wasting (9). Elevated ubiquitination, atrogin-1, and MURF1 expression, detected in C26 tumor-bearing mice undergoing muscle wasting, has also been shown to correlate with elevated myostatin expression and importantly was reversed upon treatment with sActRIIB myostatin antagonist (39).

It is important to mention that in addition to promoting the degradation of MYH and MYL, as shown here, atrogin-1 can also target eukaryotic initiation factor 3 subunit f (eIF3-f) for ubiquitination and subsequent degradation (16). Activation of

eIF3-f prevents myotube atrophy and in fact results in hypertrophy and enhanced muscle structural protein expression. Conversely, loss of eIF3-f has been shown to result in myotube atrophy (16). Thus myostatin may also promote sarcomeric protein loss through atrogin-1-mediated degradation of translation machinery, such as eIF3-f, which is consistent with the reduced protein synthesis observed following treatment with hMstn (Fig. 3E). However, as we observed enhanced ubiquitination of both MYH and MYL following treatment with hMstn (Fig. 2E), we believe that direct ubiquitination and thus degradation of sarcomeric proteins also occurs in response to hMstn treatment. Therefore, taken together, we propose that a combination of targeted degradation of sarcomeric proteins together with degradation of protein synthesis machinery may result in the sarcomeric protein loss and skeletal muscle wasting observed following treatment with hMstn.

In this paper we have described a mechanism which suggests that myostatin-induced human myotube atrophy results from reduced protein synthesis, impaired IGF/PI3-K/AKT signaling, and enhanced sarcomeric protein degradation, preferentially through SMAD3-dependent, FOXO1-mediated, activation of atrogin-1 and the ubiquitin-proteasome pathway (Fig. 5). Given that inhibition of myostatin leads to increased postnatal skeletal muscle growth, and excess levels of myostatin promotes dramatic skeletal muscle wasting, we propose that myostatin antagonists would have tremendous therapeutic value in alleviating human skeletal muscle wasting.

ACKNOWLEDGMENTS

We thank Dr. Esther Latres (Regeneron Pharmaceuticals, Tarrytown, NY) for gifting the MAFbx (atrogin-1) and MURF1 antibodies utilized in this present study. The MF 20a (MYH) monoclonal antibody developed by Dr. Donald A. Fischman and the T14 (MYL) monoclonal antibody developed by Dr. Frank E. Stockdale were obtained from the Developmental Studies Hybridoma Bank developed under the auspices of the NICHD and maintained by The University of Iowa, Department of Biology, Iowa City, IA.

DISCLOSURES

No conflicts of interest, financial or otherwise, are declared by the author(s).

AUTHOR CONTRIBUTIONS

Author contributions: S.L., P.D.G., M.S., R.K., and C.M. conception and design of research; S.L., V.M., G.B.-B., M.S., R.K., and C.M. performed experiments; S.L., M.S., R.K., and C.M. analyzed data; S.L., V.M., G.B.-B., P.D.G., M.S., R.K., and C.M. interpreted results of experiments; S.L., M.S., R.K., and C.M. prepared figures; S.L., P.D.G., M.S., R.K., and C.M. drafted manuscript; S.L., P.D.G., M.S., R.K., and C.M. edited and revised manuscript; S.L., V.M., G.B.-B., P.D.G., M.S., R.K., and C.M. approved final version of manuscript.

REFERENCES

1. Amirouche A, Durieux AC, Banzet S, Koulmann N, Bonnefoy R, Mouret C, Bigard X, Peinnequin A, Freyssenot D. Down-regulation of Akt/mammalian target of rapamycin signaling pathway in response to myostatin overexpression in skeletal muscle. *Endocrinology* 150: 286–294, 2009.
2. Baehr LM, Furlow JD, Bodine SC. Muscle sparing in muscle RING finger 1 null mice: response to synthetic glucocorticoids. *J Physiol* 589: 4759–4776, 2011.
3. Bigot A, Jacquemin V, Debacq-Chainiaux F, Butler-Browne GS, Toussaint O, Furling D, Mouly V. Replicative aging down-regulates the myogenic regulatory factors in human myoblasts. *Biol Cell* 100: 189–199, 2008.
4. Brault JJ, Jespersen JG, Goldberg AL. Peroxisome proliferator-activated receptor gamma coactivator 1alpha or 1beta overexpression inhibits

- muscle protein degradation, induction of ubiquitin ligases, and disuse atrophy. *J Biol Chem* 285: 19460–19471, 2010.
5. Clarke BA, Drujan D, Willis MS, Murphy LO, Corpina RA, Burova E, Rakhilin SV, Stitt TN, Patterson C, Latres E, Glass DJ. The E3 Ligase MuRF1 degrades myosin heavy chain protein in dexamethasone-treated skeletal muscle. *Cell Metab* 6: 376–385, 2007.
 6. Clop A, Marcq F, Takeda H, Pirottin D, Tordoir X, Bibe B, Bouix J, Caiment F, Elsen JM, Eychenne F, Larzul C, Laville E, Meish F, Milenkovic D, Tobin J, Charlier C, Georges M. A mutation creating a potential illegitimate microRNA target site in the myostatin gene affects muscularity in sheep. *Nat Genet* 38: 813–818, 2006.
 7. Furling D, Coiffier L, Mouly V, Barbet JP, St Guily JL, Taneja K, Gourdon G, Junien C, Butler-Browne GS. Defective satellite cells in congenital myotonic dystrophy. *Hum Mol Genet* 10: 2079–2087, 2001.
 8. Garcia PS, Cabbabe A, Kambadur R, Nicholas G, Csete M. Brief reports: elevated myostatin levels in patients with liver disease: a potential contributor to skeletal muscle wasting. *Anesth Analg* 111: 707–709, 2010.
 9. Gilson H, Schakman O, Combaret L, Lause P, Grobet L, Attaix D, Ketelslegers JM, Thissen JP. myostatin gene deletion prevents glucocorticoid-induced muscle atrophy. *Endocrinology* 148: 452–460, 2007.
 10. Gonzalez-Cadavid NF, Taylor WE, Yarasheski K, Sinha-Hikim I, Ma K, Ezzat S, Shen R, Lalani R, Asa S, Mamita M, Nair G, Arver S, Bhasin S. Organization of the human myostatin gene and expression in healthy men and HIV-infected men with muscle wasting. *Proc Natl Acad Sci USA* 95: 14938–14943, 1998.
 11. Gronostajski RM, Goldberg AL, Pardee AB. The role of increased proteolysis in the atrophy and arrest of proliferation in serum-deprived fibroblasts. *J Cell Physiol* 121: 189–198, 1984.
 12. Gustafsson T, Osterlund T, Flanagan JN, von Walden F, Trappe TA, Linnehan RM, Tesch PA. Effects of 3 days unloading on molecular regulators of muscle size in humans. *J Appl Physiol* 109: 721–727, 2010.
 13. Jacquemin V, Furling D, Bigot A, Butler-Browne GS, Mouly V. IGF-1 induces human myotube hypertrophy by increasing cell recruitment. *Exp Cell Res* 299: 148–158, 2004.
 14. Jinnin M, Ihn H, Tamaki K. Characterization of SIS3, a novel specific inhibitor of Smad3, and its effect on transforming growth factor-beta1-induced extracellular matrix expression. *Mol Pharmacol* 69: 597–607, 2006.
 15. Kambadur R, Sharma M, Smith TP, Bass JJ. Mutations in myostatin (GDF8) in double-muscling Belgian Blue and Piedmontese cattle. *Genome Res* 7: 910–916, 1997.
 16. Lagirand-Cantaloube J, Offner N, Csibi A, Leibovitch MP, Batonnet-Pichon S, Tintignac LA, Segura CT, Leibovitch SA. The initiation factor eIF3-f is a major target for atrogen1/MAFbx function in skeletal muscle atrophy. *EMBO J* 27: 1266–1276, 2008.
 17. Lecker SH, Jagoe RT, Gilbert A, Gomes M, Baracos V, Bailey J, Price SR, Mitch WE, Goldberg AL. Multiple types of skeletal muscle atrophy involve a common program of changes in gene expression. *FASEB J* 18: 39–51, 2004.
 18. Leger B, Derave W, De Bock K, Hespel P, Russell AP. Human sarcopenia reveals an increase in SOCS-3 and myostatin and a reduced efficiency of Akt phosphorylation. *Rejuvenation Res* 11: 163B–175B, 2008.
 19. Mammucari C, Milan G, Romanello V, Masiero E, Rudolf R, Del Piccolo P, Burden SJ, Di Lisi R, Sandri C, Zhao J, Goldberg AL, Schiaffino S, Sandri M. FoxO3 controls autophagy in skeletal muscle in vivo. *Cell Metab* 6: 458–471, 2007.
 20. McFarlane C, Plummer E, Thomas M, Henneby A, Ashby M, Ling N, Smith H, Sharma M, Kambadur R. myostatin induces cachexia by activating the ubiquitin proteolytic system through an NF-kappaB-independent, FoxO1-dependent mechanism. *J Cell Physiol* 209: 501–514, 2006.
 21. McPherron AC, Lawler AM, Lee SJ. Regulation of skeletal muscle mass in mice by a new TGF-beta superfamily member. *Nature* 387: 83–90, 1997.
 22. McPherron AC, Lee SJ. Double muscling in cattle due to mutations in the myostatin gene. *Proc Natl Acad Sci USA* 94: 12457–12461, 1997.
 23. Plant PJ, Brooks D, Faughnan M, Bayley T, Bain J, Singer L, Correa J, Pearce D, Binnie M, Batt J. Cellular markers of muscle atrophy in chronic obstructive pulmonary disease. *Am J Respir Cell Mol Biol* 42: 461–471, 2010.
 24. Reardon KA, Davis J, Kapsa RM, Choong P, Byrne E. myostatin, insulin-like growth factor-1, and leukemia inhibitory factor mRNAs are upregulated in chronic human disuse muscle atrophy. *Muscle Nerve* 24: 893–899, 2001.
 25. Sandri M, Lin J, Handschin C, Yang W, Arany ZP, Lecker SH, Goldberg AL, Spiegelman BM. PGC-1alpha protects skeletal muscle from atrophy by suppressing FoxO3 action and atrophy-specific gene transcription. *Proc Natl Acad Sci USA* 103: 16260–16265, 2006.
 26. Sandri M, Sandri C, Gilbert A, Skurk C, Calabria E, Picard A, Walsh K, Schiaffino S, Lecker SH, Goldberg AL. Foxo transcription factors induce the atrophy-related ubiquitin ligase atrogen-1 and cause skeletal muscle atrophy. *Cell* 117: 399–412, 2004.
 27. Sartori R, Milan G, Patron M, Mammucari C, Blaauw B, Abraham R, Sandri M. Smad2 and 3 transcription factors control muscle mass in adulthood. *Am J Physiol Cell Physiol* 296: C1248–C1257, 2009.
 28. Schuelke M, Wagner KR, Stolz LE, Hubner C, Riebel T, Komen W, Braun T, Tobin JF, Lee SJ. myostatin mutation associated with gross muscle hypertrophy in a child. *N Engl J Med* 350: 2682–2688, 2004.
 29. Sharma M, Kambadur R, Matthews KG, Somers WG, Devlin GP, Conaglen JV, Fowke PJ, Bass JJ. myostatin, a transforming growth factor-beta superfamily member, is expressed in heart muscle and is upregulated in cardiomyocytes after infarct. *J Cell Physiol* 180: 1–9, 1999.
 30. Stitt TN, Drujan D, Clarke BA, Panaro F, Timofeyeva Y, Kline WO, Gonzalez M, Yancopoulos GD, Glass DJ. The IGF-1/PI3K/Akt pathway prevents expression of muscle atrophy-induced ubiquitin ligases by inhibiting FOXO transcription factors. *Mol Cell* 14: 395–403, 2004.
 31. Tawa NE Jr, Odessey R, Goldberg AL. Inhibitors of the proteasome reduce the accelerated proteolysis in atrophying rat skeletal muscles. *J Clin Invest* 100: 197–203, 1997.
 32. Taylor WE, Bhasin S, Artaza J, Byhower F, Azam M, Willard DH Jr, Kull FC Jr, Gonzalez-Cadavid N. Myostatin inhibits cell proliferation and protein synthesis in C2C12 muscle cells. *Am J Physiol Endocrinol Metab* 280: E221–E228, 2001.
 33. Thomas M, Langley B, Berry C, Sharma M, Kirk S, Bass J, Kambadur R. myostatin, a negative regulator of muscle growth, functions by inhibiting myoblast proliferation. *J Biol Chem* 275: 40235–40243, 2000.
 34. Trendelenburg AU, Meyer A, Rohner D, Boyle J, Hatakeyama S, Glass DJ. myostatin reduces Akt/TORC1/p70S6K signaling, inhibiting myoblast differentiation and myotube size. *Am J Physiol Cell Physiol* 296: C1258–C1270, 2009.
 35. White ME, Allen CE, Dayton WR. Effect of sera from fed and fasted pigs on proliferation and protein turnover in cultured myogenic cells. *J Anim Sci* 66: 34–40, 1988.
 36. Wojcik S, Nogalska A, Engel WK, Askanas V. myostatin and its precursor protein are increased in the skeletal muscle of patients with Type-II muscle fibre atrophy. *Folia Morphol (Warsz)* 67: 6–12, 2008.
 37. Yarasheski KE, Bhasin S, Sinha-Hikim I, Pak-Loduca J, Gonzalez-Cadavid NF. Serum myostatin-immunoreactive protein is increased in 60–92 year old women and men with muscle wasting. *J Nutr Health Aging* 6: 343–348, 2002.
 38. Zhao J, Braut JJ, Schild A, Cao P, Sandri M, Schiaffino S, Lecker SH, Goldberg AL. FoxO3 coordinately activates protein degradation by the autophagic/lysosomal and proteasomal pathways in atrophying muscle cells. *Cell Metab* 6: 472–483, 2007.
 39. Zhou X, Wang JL, Lu J, Song Y, Kwak KS, Jiao Q, Rosenfeld R, Chen Q, Boone T, Simonet WS, Lacey DL, Goldberg AL, Han HQ. Reversal of cancer cachexia and muscle wasting by ActRIIB antagonism leads to prolonged survival. *Cell* 142: 531–543, 2010.
 40. Zimmers TA, Davies MV, Koniaris LG, Haynes P, Esqueda AF, Tomkinson KN, McPherron AC, Wolfman NM, Lee SJ. Induction of cachexia in mice by systemically administered myostatin. *Science* 296: 1486–1488, 2002.